

ENERGY PARTITIONING IN THE PRODUCTS OF ELEMENTARY REACTIONS INVOLVING OH-RADICALS*

DANIEL W. TRAINOR AND C. W. VON ROSENBERG, JR.

Avco Everett Research Laboratory, Inc., Everett, Massachusetts

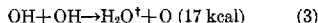
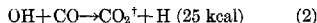
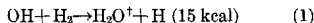
An experimental program is described in which we looked for vibrational excitation in the products of the reactions (1) $\text{OH} + \text{H}_2 \rightarrow \text{H}_2\text{O}^\dagger + \text{H}$, (2) $\text{OH} + \text{CO} \rightarrow \text{CO}_2^\dagger + \text{H}$, and (3) $\text{OH} + \text{OH} \rightarrow \text{H}_2\text{O}^\dagger + \text{O}$. No infrared emission was observed in any of the potentially radiating fundamental vibrational modes or strong combination bands of CO_2 or H_2O by our calibrated detection system, thus enabling upper bounds to be placed on the amount of vibrational excitation occurring in these products. Our results, expressed as a bound on the percent of the exothermicity which could have been deposited in the vibrational states of interest, are as follows: Reaction (1)— H_2O (2.7μ) $\leq 11\%$, H_2O (6.3μ) $\leq 18\%$; Reaction (2)— CO_2 (2.7μ) $\leq 3\%$, CO_2 (4.3μ) $\leq 0.6\%$; Reaction (3)— H_2O (2.7μ) $\leq 2\%$.

I. Introduction

The understanding of simple gas phase chemical reactions is rapidly improving as more sophisticated experiments and refined theoretical calculations explore the nature of the dynamics of the chemical interaction. By identifying the elementary processes contributing to the breaking and making of chemical bonds, we can increase our knowledge of the fundamental details of reactive collisions. Such information has been obtained from various investigations, most notably perhaps from molecular beam studies. Experiments designed to determine the extent of chemiluminescence resulting from simple reactions have also contributed significantly. The most extensively studied chemiluminescence reactions have been simple exchange reactions of the type $\text{A} + \text{BC} \rightarrow \text{AB}^\dagger + \text{C}$.¹ Specific examples of reactions of this nature are the reactions important in the HF chemical laser system: $\text{H} + \text{F}_2 \rightarrow \text{HF}^\dagger + \text{F}$ and $\text{F} + \text{H}_2 \rightarrow \text{HF}^\dagger + \text{H}$. Information concerning chemiluminescence in more complicated reactions is limited. In addition, no adequate theories exist to provide predictive capabilities and there-

fore, there is no satisfactory *a priori* means of judging whether to expect chemiluminescence behavior or not.

We report here the results of our study of energy partitioning in the elementary combustion reactions:



where the dagger (\dagger) denotes vibrational excitation, and the exothermicities indicated are for all species in their lowest energy state. Initial results of our study of the recombination reaction, $\text{O} + \text{O}_2 + \text{M} \rightarrow \text{O}_3^\dagger + \text{M}$ have already been reported.²

To make these measurements we have developed an experimental facility that couples flash photolysis with time resolved infrared detection capable of operating from 1 to 20μ . Hydroxyl radicals are produced in the experiment by the photodecomposition of H_2O vapor. Measurements of absolute OH-concentrations are obtained by time resolved resonance UV absorption spectroscopy, and infrared emission of the excited product ($\text{H}_2\text{O}^\dagger$ or CO_2^\dagger) is monitored by a calibrated IR detector which thereby gives the concentration of radiators produced. This information and

* This research was supported by the Advanced Research Projects Agency of the Department of Defense and was monitored by Space and Missile Systems Organization, Air Force Systems Command under Contract F04701-73-C-0284.

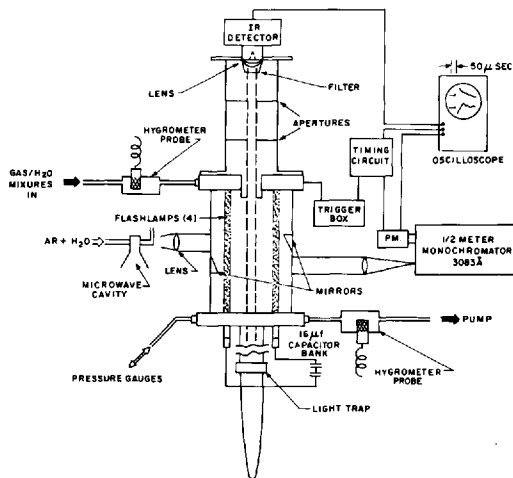


FIG. 1. Schematic drawing of experimental apparatus with IR detection and UV diagnostics.

vibrational quenching rate constants (taken from the literature) are sufficient to calculate rate constants for the reactive channels that produce vibrational excitation in the products. The time behavior of the hydroxyl radical concentration has also been reduced to provide overall rate constants for these reactions.³

II. Experimental

A. Flash Photolysis Cell

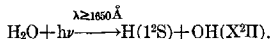
The apparatus is shown schematically in Fig. 1. The reaction cell is constructed of a quartz cylinder (13 cm ID by 22 cm) sealed by "O-rings" to two plexiglass end plates. Additional "O-ring" seals are used between the four suprasil quartz flashlamps (Xenon Corp., Medford, Mass., modified FP-6) and the bottom end plate. These flashlamps, which are wired as two pairs of two lamps in series, typically dissipate about 500 joules per discharge. This permits photo-decomposition of about 2% of the water vapor thus providing initial OH concentrations of 1 to 2×10^{14} particles/cm³. The duration of the flashlamp light pulse was measured in the ultraviolet at 2537 Å, and was found to have a full width at half maximum of approximately 8 μsec with a time to 98% extinction of approximately 31 μsec.

The test gas is supplied by a low flow rate feed system which begins with a metered reactant gas flow (H₂, CO, or N₂). A small portion of this flow is diverted through a sintered glass bubbler immersed in distilled water to generate a mixture of reactant gas + H₂O vapor. This flow is then mixed with the main flow and allowed to pass over the first of two hygrometer probes, through the cell, then over the second probe (Panometrics, Waltham, Mass., model p2) and finally to a mechanical pump. These calibrated probes provide a direct measure of water vapor partial pressure. In utilizing two probes, one upstream and one downstream of the test chamber, it was found that sufficient time (a few minutes) must be allowed following H₂O flow rate changes for the system to adjust and attain a new steady-state H₂O concentration. In this manner, water concentrations of typically 250 ± 25 microns (where the stated error represents the manufacturer's suggested accuracy for this pressure regime) were easily maintained in the cell as shown by equal readings from the two probes with agreement between the two probes of better than 10%.

Cylinder gases of the following indicated purity were used without further purification: H₂ (Liquid Carbonic, 99.95%), CO (Matheson, 99.5%), Ar (Liquid Carbonic, 99.998%) and N₂ (Liquid Carbonic, 99.998%). Total pressure in the cell was determined by a Bourdon type dial gauge (ITT, Barton) or a butyl phthalate manometer.

B. UV Absorption Diagnostic

Time resolved absorption spectroscopy was used to monitor the production and decay of the ground state OH produced by the reaction⁴



which provides the hydroxyl radicals for the experiment. A complete description of the light source and gated photomultiplier technique we used to determine absolute OH-radical concentrations has been described elsewhere.³

C. Infrared Emission Diagnostic

Since measurements in the infrared at various wavelengths between 2 to 15 μ were needed to examine the various vibrational modes involved, several infrared detectors were utilized to provide optimum detectivity at each wavelength. The detectors used were as follows: 2.7 μ , indium arsenide, (Texas Instruments, Inc.); 4.3 μ , indium antimonide, (Texas Instruments, Inc.); 6.3 μ and 15 μ , copper-doped germanium (Santa Barbara Research Laboratory, Inc.) with cold (5°K) filters. These detectors were sealed to the test cell (Fig. 1) and had appropriate wide bandpass filters and an Irtan lens. Viewing is cylindrically symmetric about the test cell's central axis and passes through a series of light baffles, through the test cell, and then into a light trap.

This arrangement of our detectors (with extensive electrical shielding, light baffling, and optical filtering) was a significant part of the development that allows us to look at background (300°K) limited IR signals as early as 20 μ sec after the flash.

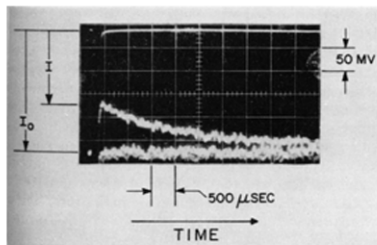


FIG. 2. Typical oscillogram showing decay of OH-absorption due to kinetic processes discussed in the text; initial mixture 0.26% $\text{H}_2\text{O} + \text{N}_2$ at 78 Torr.

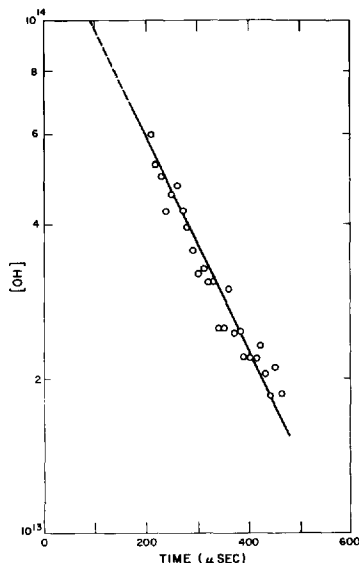


FIG. 3. Reduced data for the reaction $\text{OH} + \text{H}_2 \rightarrow \text{H}_2\text{O} + \text{H}$ obtained at H_2 pressure of 23 Torr; solid line is a fit to the data; dashed line extrapolates to $[\text{OH}]_i = 1.5 \times 10^{14}$ particles/cc.

III. Calibrations and Procedures

The use of suprasil quartz flashlamps to photolyze water vapor as a source of hydroxyl radicals to study reaction kinetics has been previously utilized.^{5,6} Our use of a gated PM to follow reaction kinetics has also been applied to reactions of the type discussed here,^{7,8} but time resolved, high sensitivity IR emission measurements have not been previously utilized on a flash photolysis experiment. The limitations of these diagnostics under flash initiation of reactions were unknown and were therefore checked experimentally.

A. UV Absorption Measurements

Measurements to assess the ability of the PM to provide accurate, reliable time histories of absolute hydroxyl radical concentrations were performed by flashing known gas mixtures and observing the OH disappearance so as to provide kinetic rate constants which could be then compared with well known literature values.

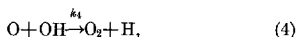
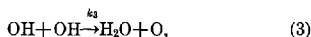
When mixtures of water vapor and nitrogen are flashed, the resultant OH radicals produced

TABLE I
 Summary of experimental results

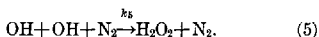
Reaction	$\text{OH} + \text{H}_2 \rightarrow \text{H}_2\text{O} + \text{H}$	$\text{OH} + \text{CO} \rightarrow \text{CO}_2 + \text{H}$	$\text{OH} + \text{OH} \rightarrow \text{H}_2\text{O} + \text{O}$	$\text{OH} + \text{OH} + \text{N}_2 \rightarrow \text{H}_2\text{O}_2 + \text{N}_2$
Leeds* value (cm^3/sec)	6.5×10^{-15}	1.55×10^{-13}	1.6×10^{-12}	No recommendation
This work	5.3×10^{-15}	1.25×10^{-13}	2.1×10^{-12}	$2.5 \times 10^{-31} \text{ cm}^3/\text{sec}$
Exothermicity (kcal/mole)	15	25	17	
Percent of exothermicity to reaction channel indicated	$2.7\mu \leq 11\%$ $6.3\mu \leq 18\%$	$2.7\mu \leq 3\%$ $4.3\mu \leq 0.6\%$ $15\mu \leq 134\%$	$2.7\mu \leq 2\%$ $6.3\mu \leq 324\%$	

* Leeds refers to Ref. 22.

follow the kinetics described by the sequence



and



The oscillogram shown in Fig. 2, obtained for an $\text{H}_2\text{O}/\text{N}_2$ mixture, illustrates the essential features of the technique. The top trace is the PM signal while the light source was blocked. The bottom trace shows the PM output with the OH lamp being monitored in the absence of OH in the test cell; these two signals provide the reference intensity, I_0 , for the absorption measurements. The third and middle trace monitors the OH absorption; it follows the unattenuated intensity of the lamp until the PM is "switched off" after which the flash occurs and the lamp intensity is attenuated due to absorption of OH radicals produced by the flash. At low pressures, such data are converted to absolute OH concentrations using the f -value and relationships presented in Ref. 9. After correction for our experimental conditions, one obtains

$$[\text{OH}] = 5.0 \times 10^{14} \log_{10}(I_0/I) \text{ particles}/\text{cm}^3.$$

Oscillograms displaying time histories of OH during reaction with H_2 and CO were also obtained. Since these reactions are first order in OH, simple plots of $\log [\text{OH}]$ vs time (see Fig. 3) provided pseudo first order rate constants from the slope. These first order rate constants are

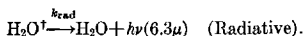
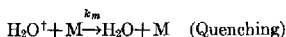
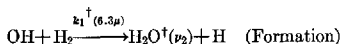
related to the desired bimolecular rate constants as follows:

$$k_I' = k_1[\text{H}_2] + \text{"constant"},$$

where the "constant" accounts for the observed decay at zero pressures of hydrogen and is due to the recombination reactions discussed above which account for <5% of the observed decay for our CO and H_2 data. Therefore, a plot of the pseudo first order rate constant, k_I' , vs $[\text{H}_2]$ gives the value for the desired bimolecular rate constant from the slope. Our data were analyzed in this manner and reasonably good agreement was found with recommended literature values (as shown in Table I).

B. IR Emission Measurements

The overall mechanism for reaction (1) producing, for example, a 6.3μ photon is described by



Under our experimental conditions, a quasi-steady state population of excited product molecules is established by the balance between the formation reaction and the quenching reactions. This population then decays in a time scale proportional to $\{k_1[\text{H}_2]\}^{-1}$ as the OH are consumed. (Although the radiative process is our principal diagnostic, it is of negligible importance (<1%) as compared to the collisional quenching process

TABLE II

Limits of Detectivity for H₂O and CO₂ in various energy states utilizing these calibrated IR detectors

Detector	In:As	In:As	In:Sb	Cu:Ge	Cu:Ge
Species	H ₂ O $\begin{pmatrix} 100 \\ 001 \end{pmatrix}$	CO ₂ $\begin{pmatrix} 101 \\ 021 \end{pmatrix}$	CO ₂ (001)	H ₂ O (010)	CO ₂ (010)
Wavelength	2.7 μ	2.7 μ	4.3 μ	6.3 μ	15 μ
Radiative lifetime	11.3 msec ¹⁰	22.6 msec ¹¹	2.27 msec ¹²	41.5 msec ¹³	668 msec ¹⁴
[Product†] for S/N=1	4.8 $\times 10^{10}$	9.6 $\times 10^{10}$	1 $\times 10^{11}$	2.4 $\times 10^{13}$	1.1 $\times 10^{14}$

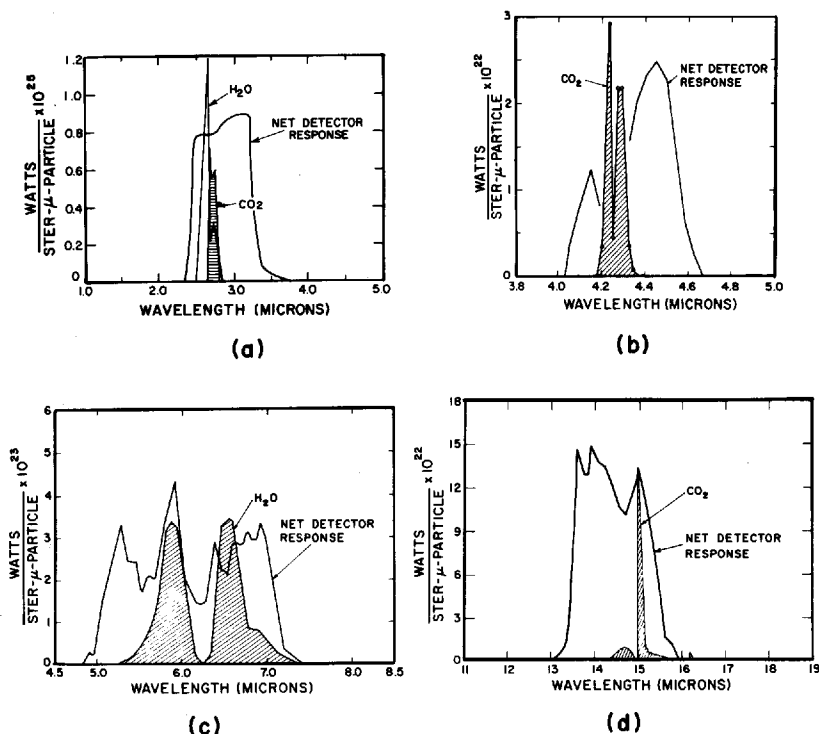


FIG. 4. (a) Room temperature emission spectrum of H₂O and CO₂ near 2.7 μ with the detection system's relative spectral response. (b) Room temperature emission spectrum of CO₂ near 4.3 μ with the detection system's relative spectral response. (c) Room temperature emission spectrum of H₂O near 6.3 μ with the detection system's relative spectral response. (d) Room temperature emission spectrum of CO₂ near 15 μ with the detection system's relative spectral response.

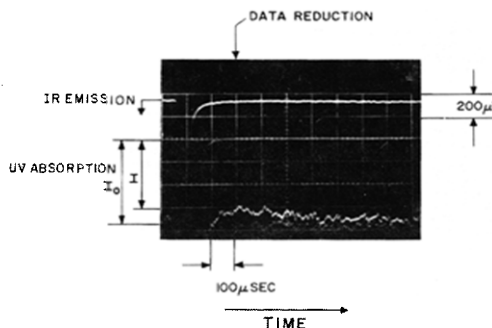


Fig. 5. Oscilloscope showing simultaneous observations in the IR and UV of the reaction $\text{OH} + \text{CO} \rightarrow \text{CO}_2 + \text{H}_2$; initial mixture 0.40% $\text{H}_2\text{O} + 1\% \text{CO} + \text{Ar}$ at 61 Torr.

in our experiment). The steady state solution for this kinetic scheme is obtained from

$$d[\text{H}_2\text{O}^+]/dt = k_1^+(6.3\mu)[\text{OH}][\text{H}_2] - \sum k_m[\text{M}][\text{H}_2\text{O}^+] = 0,$$

or

$$[\text{H}_2\text{O}^+]_{ss} = k_1^+(6.3\mu)[\text{OH}][\text{H}_2] / \sum_m k_m[\text{M}],$$

where $\text{M} = \text{H}_2, \text{H}_2\text{O}, \text{H}$, etc.

For calculation of $k_1^+(6.3\mu)$, the UV absorption diagnostic provides the concentration of OH while the other species concentrations are obtained from pressure measurements. The quenching rates are taken from the literature, and calibrated infrared detectors provide values for the concentrations of the IR radiators, in this case $\text{H}_2\text{O}(\nu_2)$ at 6.3μ .

The quenching reactions, although characterized above as a VT/VR (vibration to translation/rotation) process, are in many cases VV processes. The fastest process which acts as a drain on the mode of interest was used in reducing the data. Measurements presented in the literature for the quenching of a particular mode are sometimes known to be VT or VV and sometimes it is not known which mechanism predominates.

The infrared detectors used in the experiment were calibrated by use of a blackbody reference source (IR Industries, Inc., Waltham, Mass.; Model 101 power supply and Model 406 cavity) of known emissivity with all filters, lens, windows, apertures, etc., *in situ*. For the indium arsenide and indium antimonide detectors, the calibra-

tions were performed by imaging the detector's sensitive element into a blackbody (whose indicated temperature was checked with an ice bath reference thermocouple) with a gold plated spherical mirror. We calibrated by utilizing the difference in emission of a room temperature chopper and the blackbody (which was operated at 500 and 330°K for the 2.7μ and 4.3μ wavelengths, respectively).

Similar calibrations were also performed utilizing the Cu:Ge detector and appropriate filters, etc., but for these wavelengths a 0°C ice cooled background was constructed and signals were obtained from the room temperature mechanical chopper referenced to the cold background.

These calibration data were reduced to provide the limits of detectivity for $S/N=1$ (see Table II) for each of the important radiators in their relevant energy states. Our measurements of the spectral response of these detectors and filters are shown in Fig. 4; for comparison the room temperature emission spectrum of the relevant radiators are also displayed.

The IR detectors are sensitive to scattered photons originating with the flashlamp discharge, especially for those detector/filter combinations that have spectral overlap with the flashlamp envelope (suprasil quartz) transmission range ($<4.6\mu$) i.e., the In:As and In:Sb detectors. Their recovery was measured while viewing the reaction zone filled with an IR inactive species (N_2) during a flashlamp discharge and found to be fast compared to a reaction time.

As a check on the ability of the detectors to give reliable data immediately after recovering from the flashlamp discharge, an experiment was performed which had the detector (In:As:2.7 μ)

in situ on the reaction cell with the light trap replaced by a flat mirror which imaged the detector onto a chopper modulated blackbody. Several flashes were executed in this configuration and flashlamp pickup was found to be simply additive to the blackbody signal with recovery being complete and reproducible.

C. Typical IR Experiment

Having thus checked out both diagnostic techniques, the system was directed toward combined UV and IR measurements to provide simultaneous time resolved observations of both $[\text{OH}]$ and $[\text{product}^\dagger]$. Such an experiment is shown in Fig. 5 for the reaction of $\text{OH} + \text{CO} \rightarrow \text{CO}_2 + \text{H}$ with observations in the IR at 2.7μ .

Referring to the previously derived steady state expression, only now written to correspond to these experimental conditions, we have

$$[\text{CO}_2^\dagger]_{ss} = \frac{k_2^\dagger(2.7\mu)[\text{OH}][\text{CO}]}{k_{\text{CO}}[\text{CO}] + k_{\text{H}_2\text{O}}[\text{H}_2\text{O}] + k_{\text{Ar}}[\text{Ar}]}$$

The calibrated In:As detector, for this particular run, places a limit of $[\text{CO}_2^\dagger]_{ss} \leq 5.5 \times 10^{11}$ particles/cc at 230 μsec after the flash. The UV absorption data at the same time gives $[\text{OH}] = 5.4 \times 10^{13}$ particles/cc. Utilizing the literature values for the quenching rate constants, which are summarized in Table III, one finds $k_2^\dagger(2.7\mu) \leq 1.1 \times 10^{-14}$ cm^3/sec . By ratioing this result to the accepted overall rate constant, k_2 , one obtains the

TABLE III

Summary of vibrational quenching rate constants used in this study

Vibrational de-excitation reaction	Rate constant cm^3/sec	Ref.
$\text{CO}_2(v_2) + \text{CO} \rightarrow$	1.7×10^{-12}	15
$+ \text{H}_2\text{O} \rightarrow$	9.3×10^{-13}	16
$+ \text{Ar} \rightarrow$	2.6×10^{-13}	16, 17
$\text{CO}_2(v_2) + \text{CO} \rightarrow$	1.0×10^{-13}	18
$+ \text{H}_2\text{O} \rightarrow$	2.0×10^{-11}	17
$+ \text{Ar} \rightarrow$	1.0×10^{-13}	19
$\text{H}_2\text{O}(v_2) + \text{H}_2 \rightarrow$	1.8×10^{-13}	18
$+ \text{H}_2\text{O} \rightarrow$	5.2×10^{-12}	20
$+ \text{Ar} \rightarrow$	4×10^{-14}	20
$\text{H}_2\text{O}(v_2) + \text{H}_2 \rightarrow$	8×10^{-14}	18
$+ \text{H}_2\text{O} \rightarrow$	4×10^{-12}	20
$+ \text{Ar} \rightarrow$	6×10^{-14}	20

TABLE IV

Experimental conditions for which the results summarized in Table I were obtained

$\text{OH} + \text{CO} \rightarrow \text{CO}_2 + \text{H}$ (25 kcal)

$k^\dagger(2.7\mu)$

$[\text{OH}]_i = 6.5 \times 10^{13}$ particles/cc

$[\text{CO}] = 2.0 \times 10^{15}$

$[\text{H}_2\text{O}] = 1.0 \times 10^{15}$

$[\text{Ar}] = 2.0 \times 10^{15}$

$k^\dagger(4.3\mu)$

$[\text{OH}]_i = 7.3 \times 10^{13}$

$[\text{CO}] = 3.2 \times 10^{15}$

$[\text{H}_2\text{O}] = 1.0 \times 10^{15}$

$[\text{Ar}] = 3.2 \times 10^{15}$

$k^\dagger(15\mu)$

$[\text{OH}]_i = 1.4 \times 10^{14}$

$[\text{CO}] = 5.8 \times 10^{17}$

$[\text{H}_2\text{O}] = 9.7 \times 10^{15}$

$\text{OH} + \text{H}_2 \rightarrow \text{H}_2\text{O} + \text{H}$ (15 kcal)

$k^\dagger(2.7\mu)$

$[\text{OH}]_i = 1.1 \times 10^{14}$

$[\text{H}_2] = 7.8 \times 10^{17}$

$[\text{H}_2\text{O}] = 9.7 \times 10^{15}$

$k^\dagger(6.3\mu)$

$[\text{OH}]_i = 1.4 \times 10^{14}$

$[\text{H}_2] = 1.35 \times 10^{18}$

$[\text{H}_2\text{O}] = 7.3 \times 10^{15}$

$\text{OH} + \text{OH} \rightarrow \text{H}_2\text{O} + \text{O}$ (17 kcal)

$k^\dagger(2.7\mu)$

$[\text{OH}]_i = 1.4 \times 10^{14}$

$[\text{H}_2\text{O}] = 9.7 \times 10^{15}$

$[\text{N}_2] = 7.7 \times 10^{17}$

$k^\dagger(6.3\mu)$

$[\text{OH}]_i = 1.5 \times 10^{14}$

$[\text{H}_2\text{O}] = 9.5 \times 10^{15}$

$[\text{N}_2] = 9.7 \times 10^{17}$

quotient $k_2^\dagger(2.7\mu)/k_2 \leq 0.07$, which can be interpreted as a quantum yield. This ratio can, in principle, be greater than unity; this would correspond to more than one quantum of excitation being formed per reaction event, which is certainly energetically possible in several instances in this work. The bound on the percent of the

reaction exothermicity (E) going into 2.7μ vibration follows from $k_2^+(\lambda)/k_2 \times (hc/\lambda)/E \times 100\%$, where hc/λ is the energy of a photon at wavelength λ , in the same units as E .

In our data reduction the radiation from any band is treated as originating from a single vibrational mode with the radiative lifetimes given in Table II. In the case of $H_2O(6.3\mu)$ this is strictly true since the emission is entirely due to ν_2 mode transitions $(0n0) \rightarrow (0, n-1, 0)$. For $H_2O(2.7\mu)$ the transitions are due to both ν_1 and ν_2 with ν_2 having the shorter radiative lifetime. For $CO_2(2.7\mu)$ the transitions are due to both $(101 \rightarrow 000)$ and $(021 \rightarrow 000)$.

IV. Results and Discussion

Similar experiments were performed on reactions (1), (2), and (3) at each of the relevant wavelengths (see Table II). The results of these experiments showed no IR chemiluminescence from any of the vibrational modes of interest. By utilizing the lower limit of detectivity for these radiators as determined by the calibrated IR detectors, we are able to place an upper bound on the rate constants leading to vibrational enhancement. These results are summarized in Table I. Included in this table are the kinetic rate constant results determined in this study, the recommended literature values, and the bounds for the percent of the reaction exothermicity present in specific vibrational excitation reaction channels. The results are sensitive to the choice of vibrational relaxation rate constants (which are listed in Table III), so that as new or more reliable measurements for these vibrational quenching rates become available, these data could be re-evaluated. To facilitate this, the experimental conditions under which these limits were obtained has been summarized in Table IV. Clearly, the bounds for reaction (2) at 15μ and reaction (3) at 6.3μ are not useful. For the $OH+CO$ reaction, the limitation is due to the experimentally unfavorable wavelength for sensitive IR detection with a room temperature background and also due to the relatively long radiative lifetime involved. The $OH+OH$ experiment is insensitive because the reaction rate is second order in $[OH]$, which is produced at relatively low concentration.

It is important to note that these bounds are directly related to our measurements of absolute $[OH]$, and that we only know $[OH]$ to the extent that we know the f -value for the UV-absorption. There has been considerable controversy regarding this f -value and we discuss the rationale for our choice of Ref. 9 ($f_{00} = 7.1 \times 10^{-4}$) else-

where.³ It was originally noted,⁸ and it is generally acknowledged, that the f -value of Golden, DelGreco and Kaufman is too low if any of several assumptions were incorrect. If it is low then our estimate of $[OH]$ is high and our bounds for the percent of exothermicity into a particular mode are too low; the dependence is linear in $[OH]$ or f -value for reactions (1) and (2) and quadratic for reaction (3).

The possibility of resonance trapping by the unphotolyzed H_2O of any IR fundamental band emission from possible H_2O^+ products, formed in reactions (1) and (3), was considered as a potential source of error. The results of our experimental and theoretical efforts to evaluate this possibility are described in detail elsewhere²¹ where it is shown that self-absorption was not significant for our experimental conditions.

One explanation that is consistent with our observations on energy partitioning is that these reactions proceed via a "collision complex" which allows for equipartitioning of the available energy among the various degrees of freedom. This approach has been applied recently in other work. For example, Smith and Zellner²³ invoked collision complex formation for reaction (2) to explain the available rate data and observed activation energy and the fact that the vibrationally excited hydroxyl radicals are relaxed in non-reactive collisions with CO_2 .²⁴ In a study of the reverse reaction, translationally "hot" H-atoms were shown to react with a reasonable probability with CO_2 .²⁵ This information led them to predict little vibrational excitation would be found in the products (CO_2) of reaction (2), as is consistent with our results.

The details of collision encounters have also been studied using molecular beam techniques where product angular and velocity distributions are analyzed to obtain information on the nature of the collision interaction. Application of these techniques to the reactions described here has not been reported. However, a study of the reaction $Cs+SF_6$ showed²⁶ this reaction to proceed via a collision complex ($CsSF_6$) where the total available energy (40–50 kcal/mole) was equipartitioned among all the modes (vibration, rotation, translation). This is in contrast to the results reported²⁷ in the reaction $Li+SF_6$ where the experimental evidence indicated the reaction did not proceed via a long lived complex. Unfortunately, a reliable theory for prediction of when a "collision complex" or "sticky" collision will occur does not exist.

Application of equipartitioning of the available energy in the reactions described herein has shown that our results on reactions (1) and (3) are essentially consistent with such a distribution.

For reaction (2), however, we find substantially less emission at 2.7 and 4.3 μ than would be expected on the basis of equipartitioning. This supports the arguments of Smith and Zellner who argue that "the H-atoms should possess close to the total exothermicity of the reaction as translational energy."²²

Acknowledgment

We wish to thank Mr. Richard Ham for his contribution to developing this facility and in running the experiment.

REFERENCES

1. MTD International Review of Science, Physical Chemistry, Series One, Vol. 9, Chemical Kinetics (J. C. Polanyi, Ed.), "Chemiluminescent Reactions," by Tucker Carrington and J. C. Polanyi, p. 135.
2. VON ROSENBERG, C. W., JR., AND TRAINOR, D. W.: *J. Chem. Phys.* **59**, 2142 (1973).
3. TRAINOR, D. W. AND VON ROSENBERG, C. W. JR.: *J. Chem. Phys.* **61**, 1010 (1974).
4. CALVERT, J. G. AND PITTS, J. N., JR.: *Photochemistry*, p. 200, J. Wiley, 1966.
5. GREINER, N. R.: *J. Chem. Phys.* **46**, 2795 (1967).
6. GREINER, N. R.: *J. Chem. Phys.* **51**, 5049 (1969).
7. BAARDSEN, E. L. AND TERHUNE, R. W.: *Appl. Phys. Lett.* **21**, 209 (1972).
8. ACUNA, A. U., HUSAIN, D., AND WISENFELD, J. R.: *J. Chem. Phys.* **58**, 494 (1973).
9. GOLDEN, D. M., DEL GRECO, F. P., AND KAUFMAN, F.: *J. Chem. Phys.* **39**, 3034 (1963).
10. FERRISO, C. C., LUDWIG, C. B., AND THOMPSON, A. L.: *J. Quant. Spectrosc. Radiat. Transfer* **6**, 241 (1966).
11. FERRISO, C. C. AND LUDWIG, C. B.: *J. Opt. Soc.* **54**, 657 (1954).
12. FERRISO, C. C., LUDWIG, C. B., AND ACTON, L.: *J. Opt. Soc.* **56**, 171 (1966).
13. VON ROSENBERG, C. W., JR., PRATT, N. H., AND BRAY, K. N. C.: *J. Quant. Spectrosc. Radiat. Transfer* **6**, 241 (1966).
14. LUDWIG, C. B., FERRISO, C. C., AND ACTON, L.: *J. Opt. Soc.* **56**, 1685 (1965).
15. ROSSER, W. A., JR., SHARMA, R. D., AND GERRY, E. T.: *J. Chem. Phys.* **54**, 1196 (1971).
16. ROSSER, W. A., JR., AND GERRY, E. T.: *J. Chem. Phys.* **51**, 2286 (1969).
17. BUCHWALD, M. I. AND BAUER, S. H.: *J. Phys. Chem.* **76**, 3108 (1972).
18. Estimate.
19. SIMPSON, C. J. S. M., CHANDLER, T. R. D., AND STRAWSON, A. C.: *J. Chem. Phys.* **51**, 2214 (1969); SIMPSON, C. J. S. M. AND CHANDLER, T. R. D.: *Proc. R. Soc. Lond.* **A317**, 265 (1970).
20. KUNG, R. AND CENTER, R.: Accepted for publication, *J. Chem. Phys.*
21. A complete description of this work is available as AVCO RR #395, Avco Everett Research Laboratory, Inc., Everett, Massachusetts 02149.
22. (a) BAULCH, D. L., DRYSDALE, D. D., HORNE, D. G., AND LLOYD, A. C.: *Evaluated Kinetic Data for High Temperature Reactions*, Vol. I, Butterworths, 1972. (b) *High Temperature Reaction Rate Data No. 1*, Leeds, 1968. (c) *High Temperature Reaction Rate Data No. 2*, Leeds, 1968.
23. SMITH, I. W. M. AND ZELLNER, R.: *JCS Faraday II* **11**, 1617 (1973).
24. SMITH, I. W. M.: *Chemiluminescence and Bioluminescence*, p. 43, Plenum Press, 1973; SMITH, I. W. M. AND WOOD, P. M.: unpublished results.
25. OLDENSHAW, G. A. AND PORTER, D. A.: *Nature (Lond.)* **223**, 490 (1969).
26. RILEY, S. J. AND HERSCHBACH, D. R.: *J. Chem. Phys.* **58**, 27 (1973).
27. MARIELLA, R. P., JR., HERSCHBACH, D. R., AND KLEMPERER, W.: *J. Chem. Phys.* **58**, 3785 (1973).

COMMENTS

W. Forst, *Université Laval, Canada*. Experiments can measure the IR emission from only one CO₂ or H₂O vibrational mode at a time. Could it be that the reason for the absence of any IR emission in your experiments is the "leakage" of energy from the vibrational mode under observation into the other vibrational modes not under simultaneous observation? The intramolecular leakage or relaxation of vibrational energy is known to be quite rapid and could

easily have occurred during the initial "blind" period while your detector was recovering from the flash.

Authors' Reply. The question is relevant to the sort of experiment where the radiating species is itself formed as a direct result of the initiating energy, as for example in a laser fluorescence/vibrational relaxation experiment. This is not the case in these experiments. Rather, the flash

forms an initial concentration of OH-radicals which then react, on a much larger time scale, to form H_2O or CO_2 . If these are formed as $\text{H}_2\text{O}^\dagger$ or CO_2^\dagger then quenching reactions occur simultaneously and a quasi-steady state is established as described by the equations in Section III-B. The term "quasi-" is applied because the $[\text{OH}]$ is slowly decaying (compared to the time required to establish steady state). Indeed, there is no doubt that V-V transfer or "leakage"

occurs between modes. As a loss mechanism it is included in our formulation; while as a possible source of excitation for whatever mode is under observation, it is not included. Thus our "bounds" are, as we present them, clearly *upper* bounds on the amount of energy going into any particular mode. The experiment loses relatively little by the duration of the "blind" portion since at the point of our data reduction $[\text{OH}]$ is only slightly reduced from its value at $t_0=0$.